

Liquid phase therapy to solid electrolyte–electrode interface in solid-state Li metal batteries: A review



Chen-Zi Zhao^a, Bo-Chen Zhao^a, Chong Yan^b, Xue-Qiang Zhang^a, Jia-Qi Huang^{b,*,**}, Yifei Mo^{c,***}, Xiaoxiong Xu^{d,****}, Hong Li^{e,*****}, Qiang Zhang^{a,*}

^a Beijing Key Laboratory of Green Chemical Reaction Engineering and Technology, Department of Chemical Engineering, Tsinghua University, Beijing, 100084, China

^b Advanced Research Institute of Multidisciplinary Science, Beijing Institute of Technology, Beijing, 100081, China

^c Department of Materials Science and Engineering, University of Maryland, College Park, MD, 20742, USA

^d Ningbo Institute of Materials Technology&Engineering, Chinese Academy of Sciences, 315201, Ningbo, China

^e Institute of Physics, Chinese Academy of Science, Beijing, 100190, China

ARTICLE INFO

Keywords:

Solid-state rechargeable batteries
Electrolyte–electrode interface
Lithium metal anode
Liquid electrolyte
Solid electrolyte interface

ABSTRACT

Solid-state lithium (Li) metal batteries, employing solid electrolytes, with high energy density and enhanced safety are promising choices for next-generation electrochemical energy storage devices. However, the large interfacial resistances seriously hinder their commercialization. To construct a conformal interface with acceptable resistances, introducing small amounts of additional liquid electrolytes is one of the most convenient and effective solutions. This review summarizes the fundamental understandings on the interfacial behaviors between liquid electrolytes, electrodes and solid-state electrolytes. Afterwards, emerging strategies are discussed, involving interfacial wetting, in situ polymerization and interfacial reactions. Finally, current limitations and perspectives are presented for liquid phase therapy regarding the interfacial science and engineering.

1. Introduction

Energy is the indispensable foundation for our modern technological society. The limited reserves and environment hazards of consumed fossil fuels have evoked wide concerns, bringing the rising of renewable and environmentally friendly energy production. Taking examples of solar, wind and geothermal energy, those alternatives' intrinsic problems of discreteness in space or time require advanced energy storage and transformation. Rechargeable batteries with high energy density are one of the most promising solutions [1,2]. Among them, lithium-ion batteries (LIBs) have achieved a magnificent success in practical application, including ubiquitous portable electrical devices and the booming electric vehicles. However, the flammable organic liquid electrolytes in commercial LIBs resulted in several explosion accidents [3,4].

In place of the flammable organic liquid electrolytes, intrinsic nonflammable solid-state electrolytes (SSEs) possess the ability to

conquer the radical issues of explosion even under extreme conditions and also represent advantages of high mechanical strength, excellent chemical/electrochemical stability, wide temperature ranges and high Li-ion transference number [5–7]. The solid battery systems can be stacked within one package through alternating electrodes and solid-state electrolytes with single current collector. Consequently, weight and volume density can be much increased, especially when accompanied with lithium metal anodes [8–11].

Coexisting with above advantages, challenges of solid-state electrolytes obstruct the practical application of all-solid-state batteries, especially under room temperature. Compared with widely-used organic liquid electrolytes, the low intrinsic ionic conductivity in the bulk solid-state electrolytes at room temperature worsens the Li⁺ migration between electrodes, where numerous works have been devoted and made much progress [12–15]. For instance, sulfide electrolytes such as Li₁₀GeP₂S₁₂ (LGPS) exhibit outstanding room-temperature ionic

* Corresponding author.

** Corresponding author.

*** Corresponding author.

**** Corresponding author.

***** Corresponding author.

E-mail addresses: jhuang@bit.edu.cn (J.-Q. Huang), yfmo@umd.edu (Y. Mo), xuxx@nimte.ac.cn (X. Xu), hli@iphy.ac.cn (H. Li), zhang-qiang@mails.tsinghua.edu.cn (Q. Zhang).

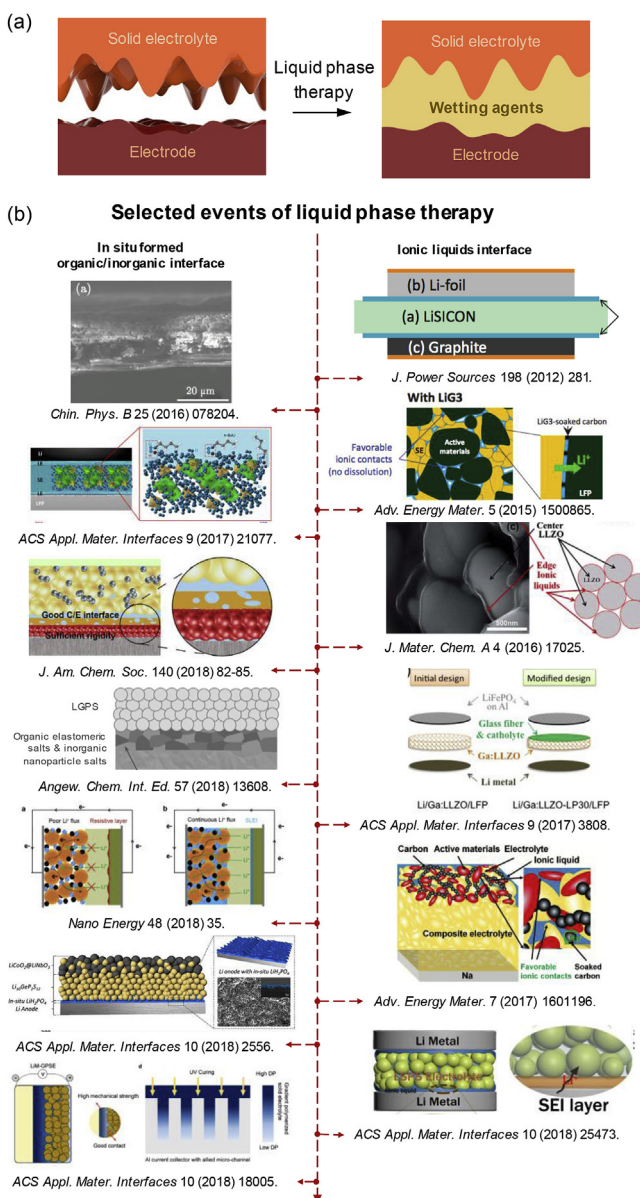


Fig. 1. Schematic diagrams and the timeline of liquid phase therapy in solid-state Li metal batteries [31–33,35,38–46].

conductivity of $10^{-3} \text{ S cm}^{-1}$, which is comparable to that of organic liquid electrolytes currently used in commercial lithium-ion systems [16]. In spite of the much-enhanced ionic conductivity, practical batteries still suffer from the limited specific capacity and shortened cycling life due to the electrons conduction capability [17], point contact of solid particles, and enlarged interfacial resistances. Therefore, it arouses increasing attention that the interfacial issues between solid-state electrolytes and electrodes are the rate-determining step for ionic transportation.

In typical solid-state batteries, the contact between solid electrolytes and electrodes is ineffective as a result of the non-conformal morphologies. The limited and uneven solid-solid interfacial contact results in inferior ion migration and Li dendrites formation on anodes [18,19]. In addition, there are generally interfacial reactions occurring between solid electrolytes and electrodes, especially for highly reactive sulfide/-oxide electrolytes and Li metal anodes [20–27]. Besides, the contacting of two materials with different chemical potential triggers the redistribution of mobile carriers near their interface, constituting the well-known space-charge layer [24,28]. The above-mentioned interfacial issues

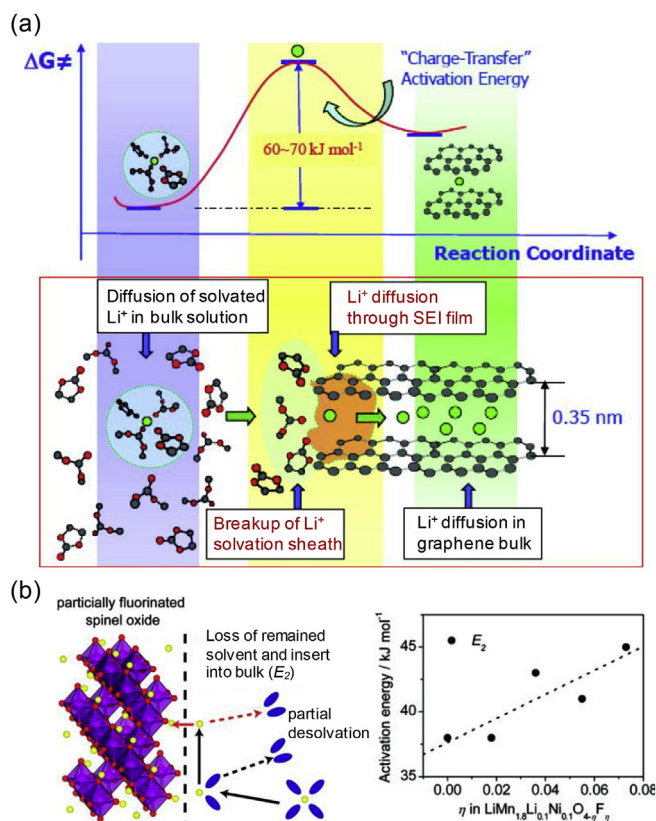


Fig. 2. Scheme of energetic coordinates for Li⁺ transfer and desolvation from electrolytes to (a) anodes and (b) cathodes [47,56].

lead to enlarged interfacial, influencing the practical energy density, cycling rate, and long-time stability.

Regarding solid-state Li metal batteries, it should be noted that there are multitudinous expressions for batteries with both solid and liquid electrolytes such as quasi-solid-state batteries [29], gel polymer electrolyte batteries [30], solid-liquid hybrid batteries [31,32], pseudo-solid-state batteries [33], dual-phase electrolyte [34] etc. In order to avoid misunderstanding, it's crucial to distinguish the ambiguous identifications and standardize the different expressions.

To improve the interfacial contact between solid-state electrolytes and electrodes, liquid phase therapy is a convenient and effective strategy to reduce the solid-solid interfacial resistances. The liquid phase therapy is introducing liquid electrolytes and related chemical/electrochemical reactions to enhance the ionic transportation and stability for the multiple interfaces in solid-state batteries, where the solid-state electrolyte is still dominating the ion transportation. Li and co-workers pioneered the work of liquid phase therapy by introducing carbonate electrolytes as the film-forming additives to in situ generate an interfacial layer between oxide solid-state electrolytes and Li metal electrodes utilizing the decomposition of organic electrolytes during cycling, which results in Li dendrite suppression and excellent cycle performances even at high rate [35]. Afterwards numerous efforts are devoted to the liquid phase therapy for interface development in lithium and sodium metal batteries [36–38].

This review focuses on batteries employing solid-state electrolytes as the main ionic conductors, with a small amount of liquid substance within the interfaces. Owing to the mobility of liquid phase, the point contact of electrodes and electrolytes can be much enhanced with liquid substances (Fig. 1).

2. Interfacial behaviors between liquid and solid substances

Liquid phase therapy introduces new interfaces in solid-state

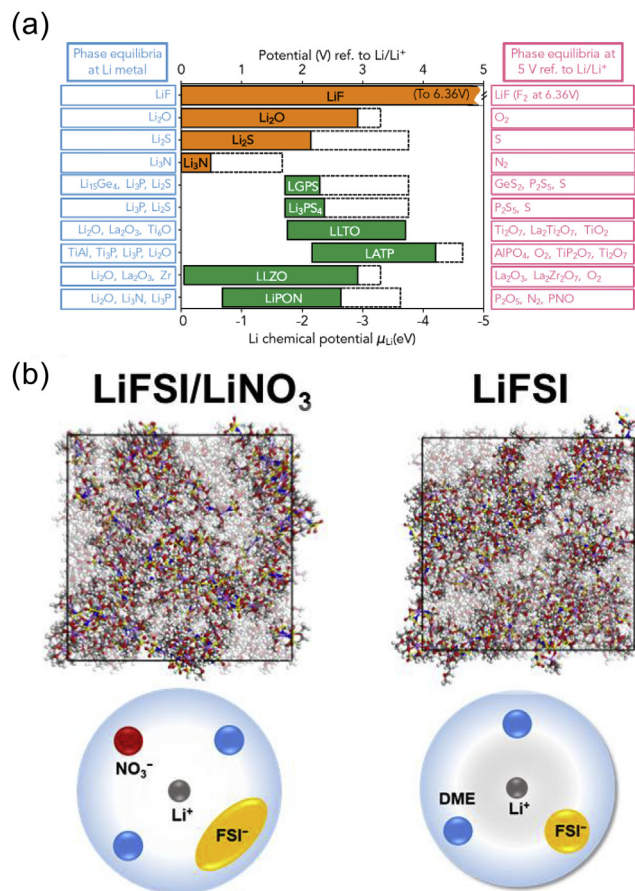


Fig. 3. Interfacial reaction properties of electrolytes. (a) Thermodynamic intrinsic electrochemical stability windows of Li salts and electrolytes. Li binary compounds (orange), selected solid electrolytes (green), and corresponding phase equilibria of the solid electrolytes at 0 V and 5 V. The dashed boxes mark the potential at which the compound is fully delithiated [23]. (b) Solvation structure of Li ions. Top panel: snapshots of the Molecular Dynamic (MD) simulation boxes of LiFSI/LiNO₃ and LiFSI electrolyte. Colors for different atoms: H-white, Li-purple, C-gray, O-red, N-blue, F-green, and S-yellow. The unsolvated solvents are in light gray. Bottom panel: schematics of the solvation structure of Li ions in corresponding electrolyte [69]. (For interpretation of the references to colour in this figure legend, the reader is referred to the Web version of this article.)

batteries, thus the interfacial behaviors between liquid substances and solid substances are of vital importance to reduce the interfacial resistances. The commonly used liquid substances are organic liquid electrolytes and room-temperature ionic liquids (RTILs). In this section, interfacial behaviors are decoupled into ionic migration and chemical reactions.

2.1. Interfacial ionic migration

The Li ions transports are altered from the migration in all solid substances to liquid-solid multiphase when fresh liquid-solid interfaces are generated due to the additional wetting agents. The process of Li⁺ transferring across a liquid/solid interface is composed of following steps (Fig. 2a) [47]: i) Li ions coordinated by several solvent molecules migrate in liquid phase with the diffusion mechanism, ii) Solvated Li ions are stripped from the solvent sheath of at the interface, iii) Li ions are transported in solid phase with respective mechanisms, such as the interstitial, collective, knock-off, vacancy and hopping mechanisms [44, 48–51]. Although the migration pathways are distinct in various systems, it is extensively accepted that the desolvation process is the rate-determining step. Consequently, the features of the coordination

structure of Li⁺ is crucial in the ionic transports. It can be inferred that a much stable coordination structure, equivalent to strong interaction between Li⁺ and solvents/anions, exhibits high activation energy barrier when dissociating to a naked Li⁺ [52]. Actually, the desolvation process is much complex due to the formation of solid electrolyte interphase on reactive electrodes. Pulse voltammetric and AC impedance spectroscopic under different ambient temperatures are effective methods to identify the charge-transfer resistance, and the activation energy can be calculated by Arrhenius formula.

Within the electrolyte system, a strong Lewis acid and a strong Lewis base generally with higher donor number contribute to higher lithium salt solubility in organics, such as tetramethylurea (TMU) and dimethyl sulfoxide (DMSO) [53]. Abe et al. claimed that for the concentrated solution, the cleavage of the ion-ion interaction is the rate-determining step [54]. In the battery systems employing both liquid and solid ionic conductors, “soggy sand electrolytes” aroused certain investigations about the second phase effects on ionic conductivity [55], where the interfacial properties of solid-state electrolytes and organic electrolytes are still lacking a widely-accepted research paradigm.

At the interfaces between organic liquid electrolytes and cathodes, the Li ions transfer resistances are mostly influenced by the solid part. The oxide cathode structures during cycling and the electrolyte decomposition layer influence the Li ions intercalation and extraction. For instance, the ions desolvation processes before entering partially fluorinated insertion electrodes (LiMn_{1.8}Li_{0.1}Ni_{0.1}O_{4-n}F_n, $\eta = 0, 0.018, 0.036, 0.055, 0.073$) consist of two steps (Fig. 2b) [56]. Firstly, solvated Li ions adsorb on the cathode surface and strip a part of solvent molecules into partially desolvated Li ions. Then they diffuse through the surface followed by the electrode incorporation of the ions with remaining solvent molecules taking off.

For electrolyte-Li metal interfaces, lithium ion migration is much more sophisticated owing to the ultrahigh reactivity of lithium metal [57, 58]. The solid electrolyte interphase (SEI) layer is created the time Li metal contacting organic electrolytes. Whether the ion desolvation process occurs before or after the electrochemical reduction is still controversial, as the SEI layer is a complex containing oligomers and inorganics. Although it is hard to determine the transportation pathway from liquid phase to Li metal anode, the solvation sheath structure and SEI component can be regulated by altering solvents, anions, Li⁺ concentration, and artificial surface layer, consequently enhancing the efficient ionic migration and uniform distribution [41, 59, 60].

Regarding the interfaces between ionic liquid and solid-state electrolytes/electrodes, Ogumi and co-workers investigated the Li⁺ transfer at the interfaces between lanthanum lithium titanate (LLT) and various ionic liquids [61], indicated the formation of contact ion pair, and draw the conclusions that interfacial activation energies are influenced by both anion and cation species, among which the effects of anions overweight. Theoretically, *ab initio* calculation was employed to investigate the interface between room-temperature ionic-liquid (RTIL) electrolyte and Li interface. The atomic and electronic structures of the interface between a Li (100) surface and 1-ethyl-3-methyl imidazolium tetrafluoroborate (EMIM-BF₄) ionic-liquid crystal was introduced as the model system. Periodic density-functional calculations revealed the significant attraction of surface Li⁺ toward BF₄⁻ anions can be counterbalanced by electron transfer toward EMIM⁺ cations near the interface, revealing the tendency of lithium ionization, Li_x-BF₄ cluster formation, and the reduction of EMIM⁺ [62].

2.2. Interfacial reaction properties

2.2.1. Interfacial reaction between liquid substance and anode

The reactions between liquid electrolytes and anodes occur on the condition that the electrochemical potentials of anode are higher than the reduction limit of electrolytes, and the reactions end until either electrons or ions are obstructed, generally due to the formation of electron insulating layer (Fig. 3a) [23, 63–66]. Theoretical calculations reveal

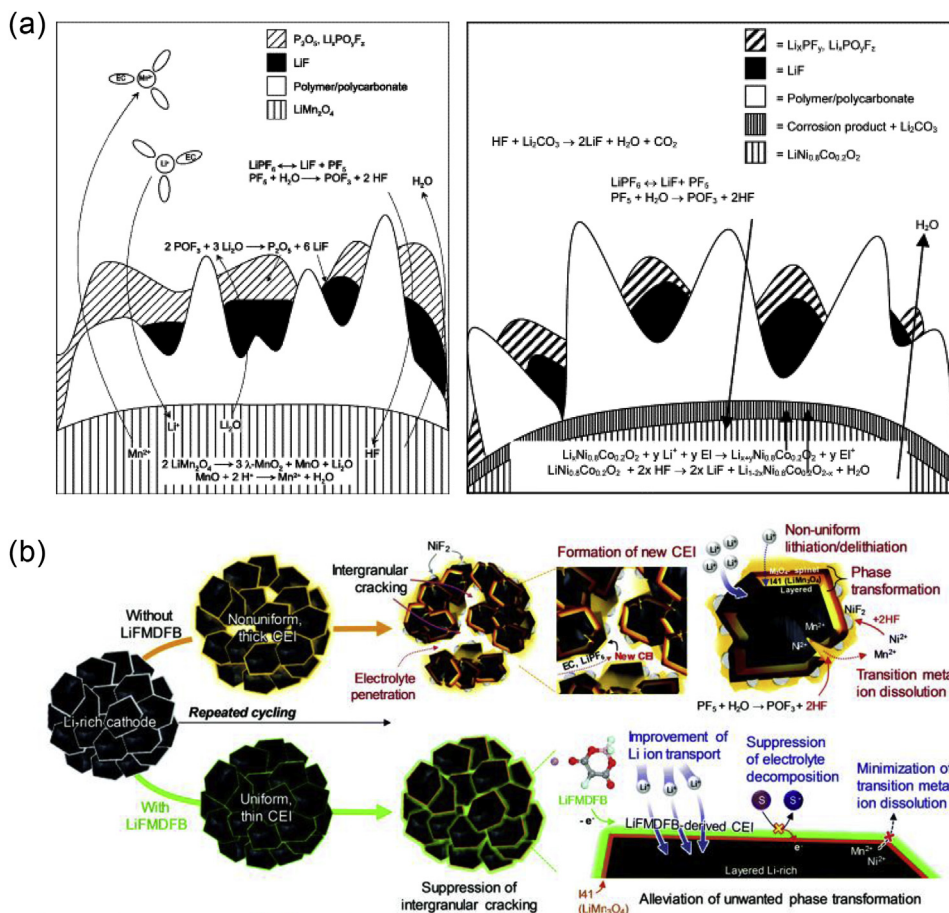


Fig. 4. Interfacial reaction between liquid substance and cathode. (a) A proposed model for the solid permeable interface surface layer formed on LiMn₂O₄ and LiNi_{0.8}Co_{0.2}O₂ electrode [77]. (b) Schematic illustration showing the positive effects of the LiFMDFB-derived CEI layer on a Li-rich cathode during repeated cycling [41].

that anions themselves are difficult to be reduced according to the enthalpy changes. Nevertheless, Li ions are coordinated with anions and solvents practically, contributing to the decreased enthalpy and the thermodynamically favorable reactions on Li metal surface [67].

Lithium metal reduction in nonaqueous electrolyte occurs in less than milliseconds after contact [68]. The generated SEI layer is heterogeneous and has aroused abundant investigations. Advanced technologies such as time-of-flight secondary ion mass spectrometer (TOF-SIMS), X-ray photoelectron spectroscopy (XPS) and nuclear magnetic resonance (NMR) present an opportunity to characterize the reactions and products, where inorganic compositions, such as Li₂O, LiF, Li₃N, LiOH and Li₂CO₃, are generally deposited approaching the anode, and organic compositions, such as ROCO₂Li, ROLi, and RCOO₂Li (R refers to organic groups related to the solvent), are gathered above the inorganic compositions. As a result, the components of SEI are dominated by the liquid electrolyte composition and the solvation structure of Li ions (Fig. 3b) [69]. Consequently, regulating the solvation structure of Li⁺ is a practical strategy to customize SEI.

SEI also generates at the interface between lithium metal anode and RTILs with different reaction activities. Considering the cations among ionic liquids, the imidazolium-based ionic liquids exhibit unsatisfying stability towards the lithium anode, due to the acidic proton at the imidazolium C-2 position. The stability can be improved by exchanging the acidic proton by a methyl group to prevent carbene formation [70,71]. Comparably, the RTILs based on tetraalkylammonium, pyrrolidinium, or piperidinium cations are more stable against reduction on lithium metal anodes [72]. Moreover, categories of anions in RTILs also highly influence the characteristics of SEI and battery performances. For instance, a

dense SEI layer with high resistance was obtained from ionic liquids containing boron tetrafluoride anions (BF₄⁻) and vinylene carbonates (VC), resulting in the dendritic lithium deposition and inferior cycling stability. On contrast, ionic liquids containing bis(trifluoromethanesulfon)imide anion (TFSI⁻) lead to a SEI layer with low interfacial resistances and superior cycling stability of around 100 cycles [73,74]. In addition, bis(fluorosulfonyl)imide anion (FSI⁻) also contributes to constructing high conductive interfacial layers [75,76].

2.2.2. Interfacial reaction between liquid substance and cathode

High-voltage cathodes have gained massive researches to realize a competitive gravimetric and volumetric energy density, such as LiNiO₂, LiNi_{1-y}Co_yO₂ ($0.1 \leq y \leq 0.3$), LiMn₂O₄, LiNi_{0.5}Mn_{1.5}O₄, etc., where a solid layer is also generated between electrolytes and cathodes, known as cathode-electrolyte interphase (CEI) (Fig. 4a) [77]. The continuous side reactions between electrolytes and cathodes bring about the electrolyte decompositions and irreversible capacity fading in the initial cycle. The existence of fluoric acid (HF) and water even accelerates the above process [78,79].

It is generally believed that CEI is an electronic insulator, but whether it is ionic conducting is controversial. Compared with SEI on the anode side, CEI is regarded much thinner with only several nanometers thick, while also renders a heterogeneous layered structure consisting of inorganic and organic compounds. In order to construct a stable CEI, sacrificial electrolyte additives are intensively employed, such as lithium bis(oxalate)borate (LiBOB), tributyl borate (TBB), Tris(pentafluorophenyl)phosphine (TPPPP), methylene methanedisulfonate (MMDS), lithium fluoromalonato(difluoro)borate (LiFMDFB), etc. The

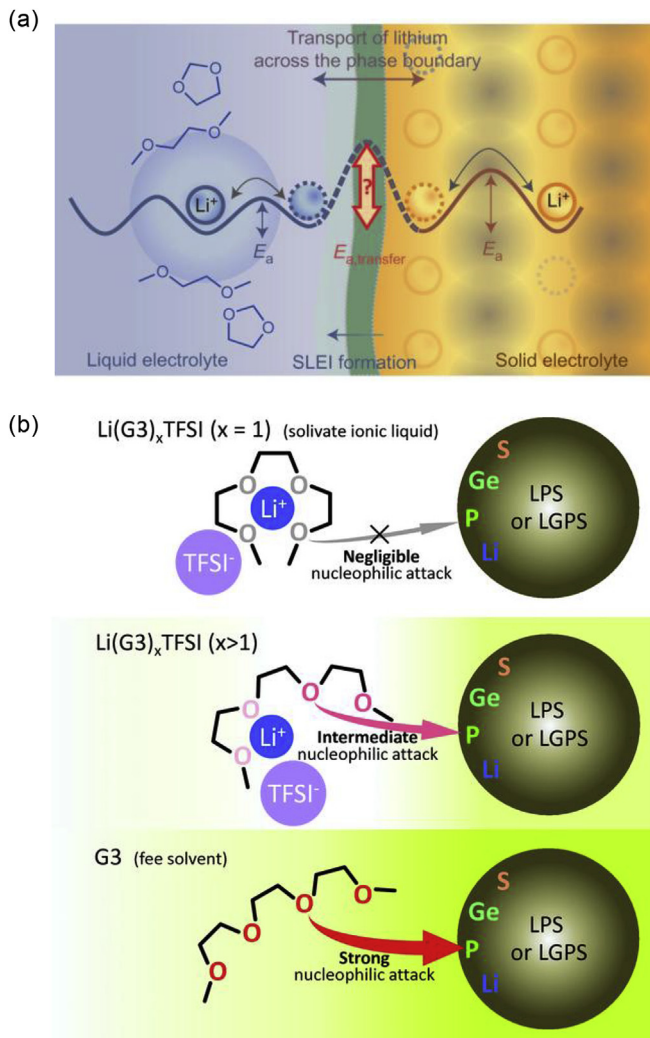


Fig. 5. Interfacial reaction between liquid electrolytes and solid-state electrolytes. (a) Ion transport across the phase boundary between a liquid electrolyte and a solid electrolyte. Activation energies, E_a , can be measured and assigned to the conduction mechanisms in both types of electrolyte. The transport of ions across the phase boundary and the SLEI contribute to the overall impedance. At least one additional activation energy can be assigned [80]. (b) Schematic diagrams representing the reactivity of glyme-based liquids (G3 and $\text{Li}(\text{G3})_x\text{TFSI}$). Note that strong coordination of Li ions by O in the glyme weakens the nucleophilic attack on electropositive elements, P, resulting in nonsolvent behavior as x in $\text{Li}(\text{G3})_x\text{TFSI}$ decreases [40].

CEI evolution with/without LiFMDFB is shown in Fig. 4b, where LiFMDFB-derived CEI exhibits enhanced stability [41]. Moreover, several high-voltage electrolytes, such as sulfone-based solvents, ionic liquids, and dinitrile solvents, are regarded to restrain the formation of CEI, while they still cannot prevent the decomposition on the Li metal anodes.

2.2.3. Interfacial reaction between liquid substance and solid-state electrolyte

The efforts dedicated to interfacial reactions between organic liquid substances and solid-state electrolytes are relatively less compared with those between the electrode interfaces. Janek and co-workers described the dynamic formation of solid-liquid electrolyte interphase (SLEI), and observed an interface film by simply immersing the liquid electrolytes onto the solid ionic conductors (Fig. 5a) [80]. $\text{Li}_{1+x}\text{Al}_x\text{Ge}_{2-x}(\text{PO}_4)_3$ (LAGP) ceramics exposed to LiTFSI (lithium bis(trifluoromethanesulfonyl)imide), DOL (1,3-dioxolane)/DME (1,2-dimethoxyethane) electrolytes forms an interface layer on ceramic surface.

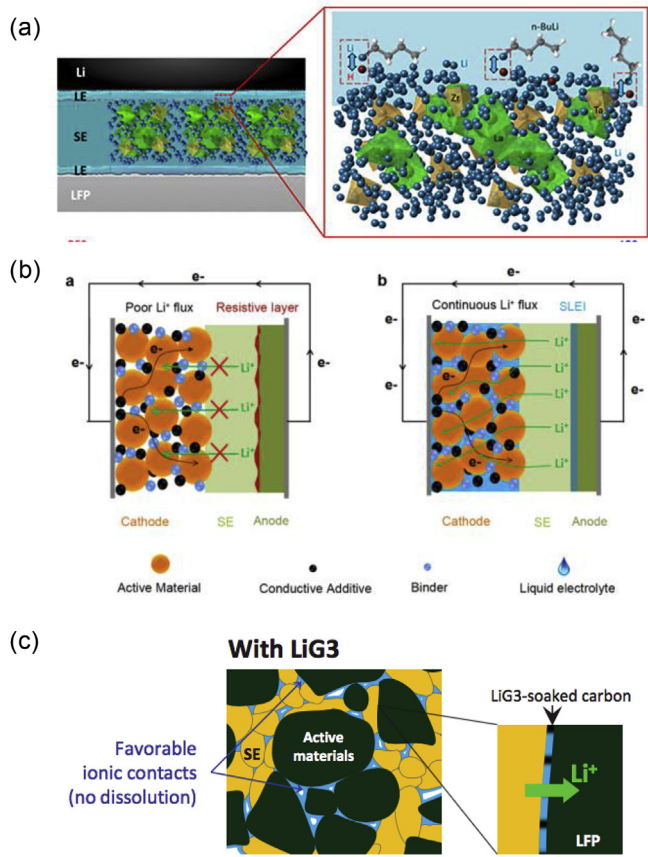


Fig. 6. Schematic diagrams of interfacial wetting. (a) Schematics illustrating the effect of $n\text{-BuLi}$ on stabilizing the SE/LE interface [32]. (b) Schematic diagram of 3D continuous Li^+ ion flux. A trace amount of LE was added to both sides of the SE, filling the pores within the cathode as well as wetting the Li metal surface [31]. (c) Schematic diagram representing the microstructure of the composite electrodes without and with LiG3, showing that LiG3 improves the imperfect solid-solid contacts. Carbon additives included in the composite electrode are not shown in the scheme [40].

Although the formation mechanism of SLEI is unclear yet, the components of SLEI can be analyzed by XPS, ToF-SIMS, Raman spectrum, etc., where inorganic compounds (i.e. LiF , CO_3^{2-} , PO_4^{3-}) and polymeric compounds can be detected. Jung and co-workers investigated the stability of sulfide solid-state electrolytes toward ionic liquids, and concluded that the Lewis alkalinity of oxygen in the triglyme (triethylene glycol dimethyl ether, G3) is weaker than oxygen in organic solvents. Hence, G3 renders a weaker trend to nucleophilic attack towards sulfide solid-state electrolyte and realized the compatibility between G3 and LPS/LGPS (Fig. 5b) [40]. The SLEI layers are generated from multiple reactions and become steady after several cycles. Compared with activation energies of Li ions transfer within the liquid and solid-state electrolytes (including grain boundaries), the charge transfer across SLEI is the rate-determining step, which increases the resistance and retards Li ions migration at the interface. The existence of water facilitates the formation of SLEI. Clearly, more researches are necessary to identify the reactions between organic liquid and solid-state electrolytes.

Overall, the interfaces between liquid and solid phase dominate the ionic transportation efficiency for SEI, CEI and SLEI. And the solvation structure of Li ions contributes much to the interfacial properties. Therefore, introducing appropriate liquid phase therapy with high mobility not only helps to increase the effective contact area between solid electrolyte and electrodes, also promotes ions migration comprehensively.

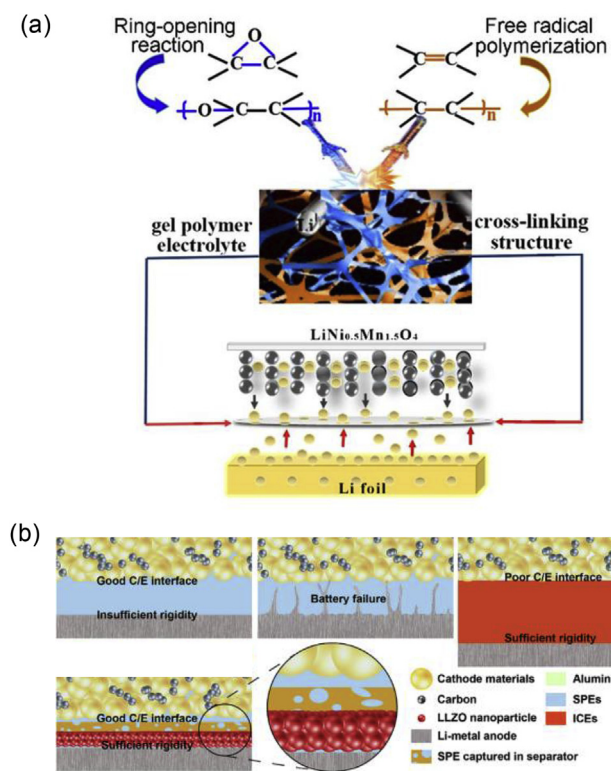


Fig. 7. Schematic diagrams of in-situ polymerization. (a) Schematics of in situ polymerization for Li metal battery [97]. (b) Schematic diagrams of solid Li-metal battery with solid polymer electrolytes (SPEs), inorganic ceramic electrolytes (ICEs) and asymmetric solid electrolytes (ASEs) Cathode/electrolyte is designated as C/E [41].

3. Strategies for liquid phase therapy

The well-developed contact strategy aims to construct conformal interfaces, including interfacial wetting, in-situ polymerization and designed interfacial reactions, keeping solid-solid interfaces contact effectively in charge and discharge process.

3.1. Interfacial wetting

The ionic transport through pristine interface between solid-state electrolyte and electrode is sluggish due to the limited contact of inflexible solid substances, especially the ceramic electrolytes with high ionic conductivity. The alternation to polymer solid ionic conductors rather than ceramics improves the flexibility of solid-state electrolyte for the increased contact area, while the inadequate ions transportation capability of polymer segments motions hinders the operation under room temperature.

In order to establish the conformal interface, interfacial wetting is one of the most convenient solutions. The point-point access is converted to much extensive area contact due to the liquid electrolyte wetting with high mobility.

The widely-used carbonate-based liquid electrolytes are favorable for wetting reagents. Aguesse, Llordés and co-workers compared the cycling performances of polycrystalline garnet-type ceramics electrolyte with or without carbonate electrolytes for interfacial wetting in full cells, where 40 μ L of 1 M LiPF₆ in EC/dimethyl carbonate (DMC) is added into a glass fiber as the wetting layer between the Li_{6.55}Ga_{0.15}La₃Zr₂O₁₂ ceramic electrolyte and LiFePO₄ cathode, facilitating the Li⁺ transfer at interface [43]. Zhong and co-workers added the carbonate-based electrolyte at interfaces between Li₇La₃Zr_{1.5}Ta_{0.5}O₁₂ (LLZT) and bipolar electrodes for Li | liquid electrolyte (LE) | LLZO | LE | LiFePO₄ configuration. Besides, it

was revealed that the Li^{+/H⁺} exchange might lead to Li⁺ deficiency along the LE/LLZO interface and retard Li⁺ conduction, thus they added n-BuLi, a super base, into LE to restrict Li^{+/H⁺} exchange and lithiate LE/garnet interface (Fig. 6a) [32]. Further, Sun and co-workers cut down the volume of LE to 2 μ L at both interfaces. The LE added at cathode/Li_{1.4}Al_{0.4}Ti_{1.6}(PO₄)₃ (LATP) interface acted as wetting reagent to form an intermediate layer on the cathode and dense SLEI approaching the anode, enabling the continuous Li ions flux and preventing the reduction of LATP by Li metal (Fig. 6b) [31]. Although the carbonate-based liquid electrolytes render numerous benefits such as low cost and universality, the poor chemical stability against strong reductive/oxidative electrodes results in severe consumption of LE and subsequently shortened cycle life. While, it generates safety concerns again if excess organic electrolytes are employed to compensate for the consumption, obstructing their applications.

RTIL constitutes another candidate for interfacial wetting owing to its high ionic conductivity, thermal stability, nonvolatility, nonflammability and excellent stability against electrodes and solid-state electrolytes. RTILs have been mixed into polyethylene oxide (PEO)-based polymeric electrolytes for flexible composite electrolytes with promoted interfacial contact [81,82]. In general, RTILs are mostly coupled with oxides, such as LISICON-type, NASICON-type, garnet-type solid-state electrolytes to reduce resistance at Li/SSE, graphite/SSE, cathode/SSE interfaces [33, 38,39,83]. Sodium batteries also provide inspirations for lithium metal batteries [84]. Nonvolatile and nonflammable ionic liquids such as anion-based N-methyl-N-propyl-piperidinium-bis(fluorosulfonyl) imide (PP13FSI) can be also utilized for solid-state sodium batteries. The ionic liquid-wetted batteries can be operated at room temperature and exhibit prolonged cycling lifetime (250 cycles vs. 40 cycles) compared with the all-solid-state batteries operating at 80 °C [38]. Moreover, Goodenough and co-workers also employed the plastic-crystal electrolytes constituted by succinonitrile complexed with sodium salts to penetrate into the cathodes for larger access [37]. Guo and co-workers synthesized a composite electrolyte consisting of Li-salt-free PEO and Li_{6.4}La₂Zr_{1.4}Ta_{0.6}O₁₂ (LLZTO) wetted by 1.8 μ L cm⁻² [BMIM]TF₂N in interface. Solid-state Li metal full cells realized competitive rate capability and stability. Numerous Li ions are released from LLZTO and transported through abundant conductive paths through the RTIL wetted interfaces [82]. Meanwhile, Zhang and co-workers proposed that dissolving a lithium salt in RTIL for enhanced ionic conductivity will inevitably lead to stronger ionic interactions in the mixture, which increases the viscosity and hence affects the ionic mobility. Hence, 1-butyl-1-methylpyrrolidinium bis(trifluoromethylsulfonyl) imide (BMP-TFSI) was added to not only facilitate Li⁺ transfer at interface, also suppress lithium dendrite growth by homogenizing Li ions distribution [85]. However, Appetecchi and co-workers doubted whether NASICON-ionic liquid hybrid electrolytes can realize a synergic effect to accelerate ionic transportation [86]. They claimed that simply combining Na₃Si₂Y_{0.16}Zr_{1.84}O₁₂ and N-butyl-N-methylpyrrolidinium bis(trifluoromethanesulfonyl)imide (Py₁₄TFSI) does not result in the enhancement practically due to the high activation energy barrier at interface, and processing conditions affect the ions migration. Besides oxides, ionic liquids can also be employed in sulfide electrolytes to eliminate ionic isolated particles. Jung and co-workers employed Li(G3) TFSI (triethylene glycol dimethyl ether, G3) into the composite cathodes including LiFePO₄ and carbon additives to achieve favorable ionic contacts (Fig. 6c) [40].

Therefore, interfacial wetting facilitates ions transportation effectively, but shortcomings still exist. The consumption of the limited wetting reagent is inevitable during cell cycles, leading to the conformal interface failure and battery performance decay. The intrinsic high reactivity of lithium metal and high-voltage cathodes leads to complicated interfacial reactions. A generated electron insulated layer will terminate the reactions, while a mixed ionic and electronic layer will result in severe side reactions and active materials consumption. Introducing such small amount of electrolyte addition for large-format cells

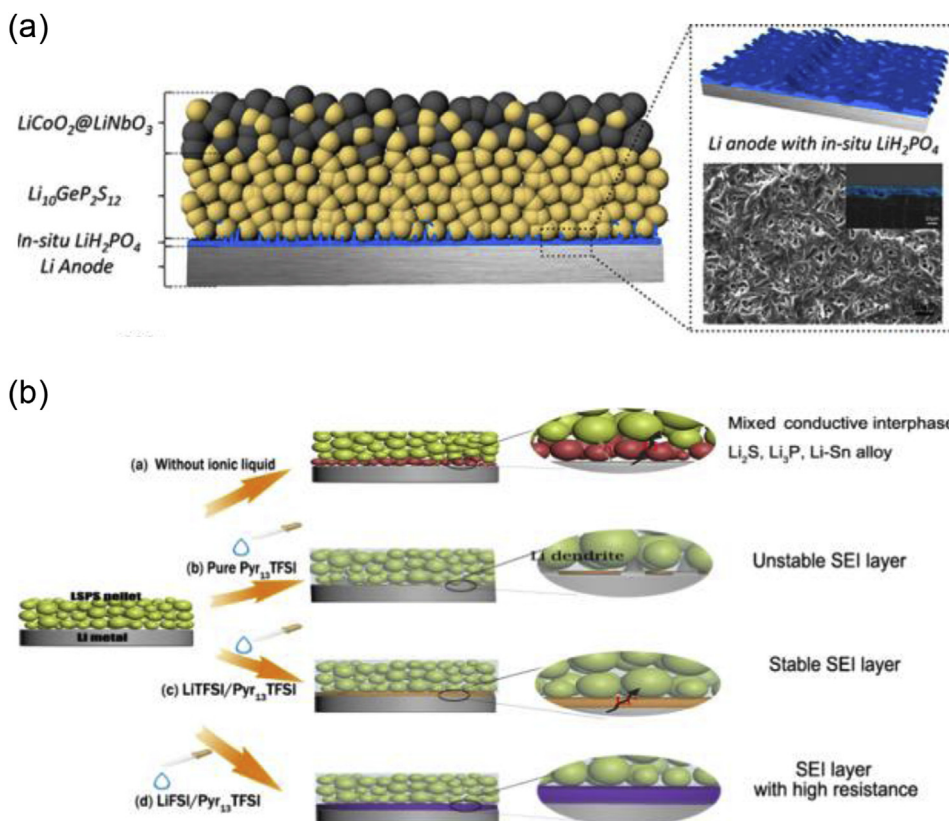


Fig. 8. Schematic diagrams of interfacial reaction. (a) Schematic of the preparation process of in situ LiH₂PO₄ protective layer and the LCO/LGPS/LiH₂PO₄-Li battery with optimized structure [44]. (b) Schematic illustration of interfacial modification mechanism of different Li salts and Pyr₁₃TFSI [45].

requires the innovation in terms of manufactory for quality control purposes. In addition, the intrinsic energy barrier at the solid-liquid interfaces and the high cost of RTILs should also be concerned. In order to take advantage of interfacial wetting, it is vital to decrease the migration barrier of the fresh interface, increase the compatibility of wetting reagents and reduce the cost of fabrication.

3.2. In-situ polymerization

A stable conformal interface for ionic conduction requires a deformable interfacial layer to tolerate huge volume changes during repeated cycling, where in situ polymerization leads to a native and flexible conformal interface to fit the intrinsic morphology of electrode and electrolytes [87]. Polymer precursors are favorable for maximizing the contact area, then in-situ polymerization is triggered to fulfill the inter-space under certain conditions, such as thermal initiation, ultraviolet ray (UV) and electricity [46,88–90]. Although several strategies of in-situ polymerization are not formerly presented to solve the inorganic electrolyte-electrode interfaces, they offer significant opportunities for future interface engineering and will also be reviewed in this section.

Recently, Kang and co-workers carried out a series of researches about in-situ polymerization, such as polyaniline (PANI), poly(ethylene glycol) diglycidyl ether (PEGDE), polyvinyl alcohol (PVA), and pentaerythritol tetraacrylate (PETEA)-based gel polymer electrolyte [91–93]. For instance, Zhou et al. revealed that the in-situ gelation mechanism of cyanoethyl polyvinyl alcohol (PVA-CN) based gel polymer electrolyte is actually the in-situ cationic polymerization of cyano resin initiated by PF₅, which is a strong Lewis acid decomposed from LiPF₆ [94]. Besides, the SiO₂ hollow nanosphere-based composite solid electrolyte is synthesized via in-situ polymerizing the tripolyphosphate glycol diacrylate (TPGDA) absorbed in SiO₂ a hollow nanosphere layer [93]. Watanabe and co-workers prepared a gradient structured poly(pyrrole)

(Ppy)/ion-conducting polymer electrolyte (PE) composites by in-situ electropolymerization, in which Ppy acted as a conductive polymer cathode and PE acted as solid-state electrolyte [95]. Zhou and co-workers found that once an appropriate current was applied during the charging-discharging processes of Li | DOL/DME | LiCO₂ cell, the original liquid electrolyte was generally polymerized during the first several cycles irreversibly [96]. Cui and co-workers investigated a series of in-situ synthesized polymer electrolytes for high-voltage operations, such as the poly(acrylic anhydride-2-methyl-acrylic acid-2-oxirane-ethyl ester-methyl methacrylate) (PAMM)-based electrolyte with in-situ cross-linking polymer network, whose electrochemical window is as extended as 5 V. The anhydride and acrylate groups can respectively provide high voltage resistance and fast ionic conductivity (Fig. 7a) [97]. Recently, Wan, Guo and co-workers put forward the concept of asymmetric solid-state electrolyte. Electrolytes on the Li metal anode side exhibit high modulus to suppress Li dendrites, and cathode-side electrolytes are flexible to reduce interfacial resistances. Batteries render an asymmetric architecture in which a rigid ceramic layer modified with a 7.5 nm-thick polymer faces Li anode and a soft polymer layer spreads over the exterior and interior of cathode, and the interior polymer layer is in-situ generated from poly(ethylene glycol) methyl ether acrylate (PEGMEA) (Fig. 7b) [41].

Consequently, in-situ polymerization can construct the conformal interface for the smooth charge transfer at the interfaces. However, the polymerization procedure is hard to control inside the battery due to the complicated chemical environment. Even if the in-situ formed polymer buffer layer offers perfect protection initially, the physical adhesion between active materials and electrolytes cannot guarantee an efficient interfacial ion migration and avoid solid separation during the entire lifecycle, especially when the volume and morphology of electrodes change tremendously in the charge and discharge process, challenging the long-term cycling.

Table 1

Comparison of solid-state battery results with and without liquid electrolyte additives.

Electrolyte	Liquid agents	Cathode/Anode	Solid-state battery results	
			with liquid electrolyte additives	without liquid phase therapy
LGPS	Li(G3) TFSI (triethylene glycol dimethyl ether, G3)	LFP (LiFePO ₄)/Li-In	144 mA h g ⁻¹ (initial) 0.1C, 30 °C 30 cycles	Negligible capacity [40]
LGPS LiSnPS	DOL/DME electrolyte 1.5 M LiTFSI/Pyr13TFSI in situ reaction	TiS ₂ /Li metal LFP/Li metal	Capacity retention of 91.7% in 200 cycles 144 mA h g ⁻¹ (initial) 0.1C	Capacity retention of 76.1% in 70 cycles [42] 103 mA h g ⁻¹ (initial) 0.1C
LGPS	LiH ₂ PO ₄ layer via H ₃ PO ₄ and Li reaction	LiCoO ₂ /Li metal	Capacity retention 84.7% after 30 cycles 118.7 mA h g ⁻¹ (500th) 0.1 C Capacity retention 86.8%	Exhibiting failure in 7 cycles [45] /[44]
LLZO	carbonate-based electrolyte with n-BuLi	LFP/Li metal	400 cycles with nearly constant interface areal resistance. 100 and 200 μA cm ⁻² room temperature	Interface resistance increasing from ~1056 to ~2419 Ω cm ⁻² after 10 cycles [32]
LATP	2 μL 1 M LiPF ₆ EC/DMC/DEC	LFP/Li metal	Interfacial resistance: 90 Ω	Interfacial resistance: 4470 Ω [31]
PEO and LLZTO	1.8 μL cm ⁻² [BMIM]TF ₂ N	LFP/Li metal	133.2 mA h g ⁻¹ 0.1C, 25 °C	/[82]
LLZTO	BMP-TFSI without lithium salts	NCM811/Li metal	Capacity 88% after 150 cycles 150 mA h g ⁻¹ (initial) 0.5C 102 mA h g ⁻¹ (200th)	/[85]
LLZO	PEGMEA	LFP/Li metal	160.6 mA h g ⁻¹ (initial) 0.2C, 55 °C 151.2 mA h g ⁻¹ (120th)	/[41]

LGPS, Li₁₀GeP₂S₁₂; LiSnPS, Li₁₀SnP₂S₁₂; LLZO, Li₇La₃Zr_{1.5}Ta_{0.5}O₁₂; LLZTO, Li_{6.4}La₃Zr_{1.4}Ta_{0.6}O₁₂; LATP, Li_{1.4}Al_{0.4}Ti_{1.6}(PO₄)₃.

3.3. Designed interfacial reaction

In order to strengthen the interaction between solid-state electrolyte and electrodes for a stable and long-term cell cycling, it is rewarding to take advantages of interfacial reaction to in situ construct the intimate contact. An ideal interlayer is a favorable ionic conductor to carry ions smoothly with tight contacts of both sides and decreased resistances, and electron insulated to avoid further corosions.

Nowadays, utilizing the interfacial reactions is still a challenge with several attempts to prevent undesirable reactions by introducing designed in situ reactions, due to that the reactions are too complicated to regulate, especially in pouch cells [98–100]. Gao et al. constructed an organic-inorganic nanocomposite interlayer via in situ electrochemical decomposition of DOL/DME electrolyte between Li metal and LGPS. The in situ formed protective layer was composed of organic elastomeric salts (LiO-(CH₂O)_n-Li) and inorganic nanoparticle salts (LiF, -NSO₂-Li, Li₂O) to protect LGPS against Li metal corrosion [42]. Xu and co-workers spin-casted the phosphoric acid (H₃PO₄) and tetrahydrofuran (THF) solution onto the Li foils to form a LiH₂PO₄ interlayer between Li and LGPS,

which not only provides an intimate contact, also eliminates the inferior reactions (Fig. 8a) [44].

Interfacial engineering including artificial SEI construction has been extensively investigated in the liquid Li metal batteries and acts as a significant reference for solid-state batteries [101,102]. Various electrolytes and additives, such as fluoroethylene carbonate (FEC), polysulfides, lithium nitrates, etc. [69], are also candidates for adjusting interfacial reactions to manipulate the interface composition and structure. Zheng et al. investigated the reactions of Li₁₀SnP₂S₁₂ (LSPS), Li metal anode, and additional ionic liquid N-propyl-N-methyl pyrrolidinium bis(trifluoromethanesulfonyl)imide (Pyr13TFSI), where an in-situ formed interface layer was established through LiTFSI/Pyr13TFSI. They also propose that LiFSI results in LiF enrichment between LSPS and Li metal, leading to higher resistance (Fig. 8b) [45].

Accordingly, strategy of regulating interfacial reactions in solid-state batteries is in infancy. Published works generally focused on forming an inert interlayer to prevent the inferior reactions efficaciously between solid-state electrolytes and electrodes. The cycling lifetime of solid-state batteries, especially under high current density and high areal capacity, is

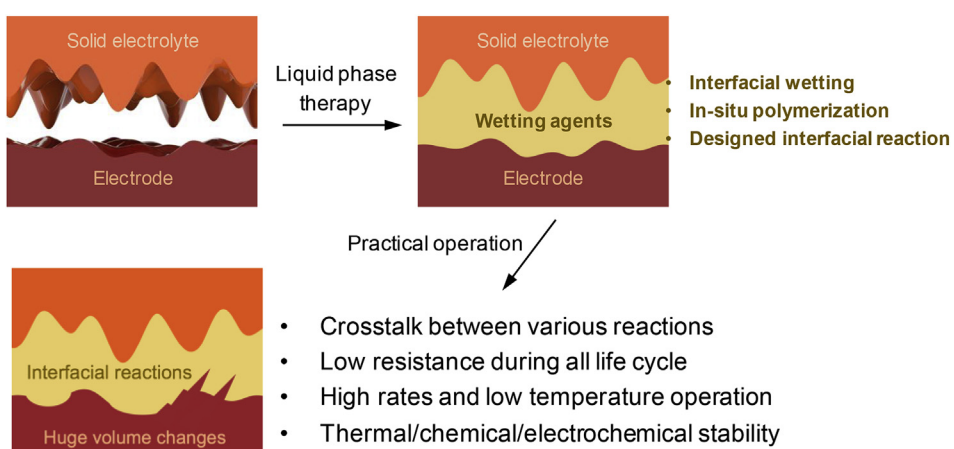


Fig. 9. Schematic diagrams and future challenges of liquid phase therapy in practical solid-state Li metal batteries.

still limited and far from practical applications. Actually, reaction principles of liquid electrolytes, solid-state electrolytes, and Li metal anodes have not been revealed clearly yet. Reactions between solid electrolyte and electrode are equally critical as many such solid-solid interfaces are chemically and electrochemically unstable, leading to a crosstalk between the various reaction pathways. The surface property of one solid-state electrolyte also varies due to the decomposition under ambient atmosphere. Therefore, a deeper understanding of the interfacial chemistry, especially material evolutions during cycling, is essential for interfacial reaction regulations.

4. Conclusion and perspective

Advanced batteries utilizing solid-state electrolytes and Li metal anodes provide significant opportunities towards high energy density and safety assurance. With the rapid development of solid-state super-ionic conductors exhibiting high ionic conductivity, the interfacial challenges constitute an increasing significant factor in battery systems. The large interfacial resistance owing to the point-point contact of solid electrolytes and electrodes retards ionic transportation, influencing the capacity, rate performance and battery lifespan.

Consequently, taking advantages of liquid phase with high mobility contributes to constructing a conformal interface layer for efficient ionic migration, where organic liquid electrolytes and room-temperature ionic liquids are generally utilized. Fortunately, there are wider choices of electrolytes for liquid therapy, as the electrochemical window can be slightly narrowed thanks to the solid electrolyte separation. The liquid phase therapy can be achieved by introducing an additional wetting process or modifying the drying process in terms of manufacturing, which can integrate into existing production lines. In this review, we summarized recent progress for understanding ion migration mechanisms and the interactions between additional liquid substances, cathodes, anodes and solid electrolytes. Multiple techniques are employed to reveal the interface evolution, where the solvation structure of Li ions is crucial in interface layer formation and rate-determine step. Based on the fundamental investigations, strategies such as interfacial wetting, in situ polymerization and designed interfacial reactions were proposed and made much progress in battery performance enhancements (Table 1). It should be noted that introducing flammable liquid substances will also increase the safety risks. Consequently, it is of vital importance to reach the balance between safety and high energy/power density requirements.

Liquid phase therapy exhibits bright prospects in interfacial engineering towards a practical Li metal battery with solid-state electrolytes. Further researches are necessary to realize a controllable interface for cell operations (Fig. 9).

- (1) Challenges and requirements for future solid-state Li metal batteries include low interfacial resistance during all life cycle, Li dendrite inhibition at high rates, high thermal/chemical/electrochemical stability, and acceptable performances at low temperature.

Practically, it is difficult to wet all active particles and restrict the liquid agents within the interfaces through limited amount of liquid electrolyte. The electrochemical stabilities of wetting reagents are still necessary for desirable CEI and SEI formation. The chemical and thermal stabilities are influenced by various components in wetting reagents such as solvents, salts, and polymers. It is rewarding to initially construct a SEI/CEI layer followed by a polymerization process, where polymers with super-elasticity is promising to tolerate huge volume changes. The liquid reagents can be transformed to solid phase through solvent evaporation and reactions in a working battery.

- (2) Accurate energy chemistry mechanisms. Fundamental science about the interfacial chemistry underpinning liquid phase therapy offers principles and innovations for practical interface design. It

is beneficial to characterize and study the interface materials and energy chemistry in solid-state Li metal batteries, especially under a large capacity and current density. It provides more opportunities to incorporate the theoretical methods (e.g. density functional calculation, phase field simulation) and advanced characterizations (e.g. in situ and operando techniques).

- (3) The development of computational modeling, machine learning, and data-driven techniques can contribute to the electrolyte screening, greatly accelerating the interface design.
- (4) Construction of a conformal interface operating effectively during whole battery lifecycle. Although amounts of strategies manage to realize a perfect interface in the initial cycle, the material revolutions might result in much increased interface resistances during repeated cycling.
- (5) Researches of solid-electrolyte interphase (SEI) layer in liquid Li metal batteries provide abundant inspirations for liquid phase therapy, while the compatibility of solid-state electrolytes and cathodes deserve sufficient attentions.
- (6) Safety concerns and cost. The introduction of excessive organic liquid electrolytes brings about safety concerns in traditional lithium metal batteries. More investigations and optimizations are required to balance the energy density, lifespan and safety. Besides, liquid phase such as ionic liquids will inevitably lead to cost increase and more sophisticated battery construction during commercialization.
- (7) Achieving a satisfying battery performance requires a full picture of battery system, where each component is indispensable, including electrode and electrolyte materials, process routings and battery operations. Consequently, it is crucial to make joint efforts in materials science, electrochemistry, chemical engineering, and abundant related fields.

Despite the challenges, liquid phase therapy is one of the most convenient and effective solutions for interface construction in lithium metal batteries. Devoting more efforts are rewarding to boost the progress. The synergism of electrochemistry, materials evolution, and interface engineering is promoting the development of practical solid-state Li metal batteries in the future.

Acknowledgements

This work was supported by the National Key Research and Development Program (2016YFA0202500 and 2016YFA0200102), the National Natural Science Foundation of China (21676160, 21776019 21825501, and U1801257), and the Tsinghua University Initiative Scientific Research Program.

References

- [1] S. Chu, A. Majumdar, *Nature* 488 (2012) 294.
- [2] X.-B. Cheng, R. Zhang, C.-Z. Zhao, Q. Zhang, *Chem. Rev.* 117 (2017) 10403–10473.
- [3] M. Asadi, B. Sayahpour, P. Abbasi, A.T. Ngo, K. Karis, J.R. Jokisaari, C. Liu, B. Narayanan, M. Gerard, P. Yasaei, X. Hu, A. Mukherjee, K.C. Lau, R.S. Assary, F. Khalili-Araghi, R.F. Klie, L.A. Curtiss, A. Salehi-Khojin, *Nature* 555 (2018) 502.
- [4] X. Lei, X. Liu, W. Ma, Z. Cao, Y. Wang, Y. Ding, *Angew. Chem. Int. Ed.* 57 (2018) 16131–16135.
- [5] L. Fan, S. Wei, S. Li, Q. Li, Y. Lu, *Adv. Energy Mater.* 8 (2018) 1702657.
- [6] C. Yang, K. Fu, Y. Zhang, E. Hitz, L. Hu, *Adv. Mater.* 29 (2017) 1701169.
- [7] C. Sun, J. Liu, Y. Gong, D.P. Wilkinson, J. Zhang, *Nano Energy* 33 (2017) 363–386.
- [8] C.-Z. Zhao, X.-Q. Zhang, X.-B. Cheng, R. Zhang, R. Xu, P.-Y. Chen, H.-J. Peng, J.-Q. Huang, Q. Zhang, *Proc. Natl. Acad. Sci. U.S.A.* 114 (2017) 11069–11074.
- [9] D. Lei, K. Shi, H. Ye, Z. Wan, Y. Wang, L. Shen, B. Li, Q.-H. Yang, F. Kang, Y.-B. He, *Adv. Funct. Mater.* 28 (2018) 1707570.
- [10] J. Yue, M. Yan, Y.-X. Yin, Y.-G. Guo, *Adv. Funct. Mater.* 28 (2018) 1707533.
- [11] Q. Zhao, X. Liu, S. Stalin, K. Khan, L.A. Archer, *Nat. Energy* 4 (2019) 365–373.
- [12] F. Mizuno, A. Hayashi, K. Tadanaga, M. Tatsumisago, *Adv. Mater.* 17 (2005) 918–921.
- [13] Y. Seino, T. Ota, K. Takada, A. Hayashi, M. Tatsumisago, *Energy Environ. Sci.* 7 (2014) 627–631.

- [14] N.-W. Li, Y.-X. Yin, C.-P. Yang, Y.-G. Guo, *Adv. Mater.* 28 (2016) 1853–1858.
- [15] J. Li, Y. Lin, H. Yao, C. Yuan, J. Liu, *ChemSusChem* 7 (2014) 1901–1908.
- [16] N. Kamaya, K. Homma, Y. Yamakawa, M. Hirayama, R. Kanno, M. Yonemura, T. Kamiyama, Y. Kato, S. Hama, K. Kawamoto, A. Mitsui, *Nat. Mater.* 10 (2011) 682.
- [17] F. Han, A.S. Westover, J. Yue, X. Fan, F. Wang, M. Chi, D.N. Leonard, N.J. Dudney, H. Wang, C. Wang, *Nat. Energy* 4 (2019) 187–196.
- [18] C. Yan, Y.-X. Yao, X. Chen, X.-B. Cheng, X.-Q. Zhang, J.-Q. Huang, Q. Zhang, *Angew. Chem. Int. Ed.* 130 (2018) 14251–14255.
- [19] K. Kerman, A. Luntz, V. Viswanathan, Y.-M. Chiang, Z. Chen, *J. Electrochem. Soc.* 164 (2017) A1731–A1744.
- [20] P. Hartmann, T. Leichtweiss, M.R. Busche, M. Schneider, M. Reich, J. Sann, P. Adelhelm, J. Janek, *J. Phys. Chem. C* 117 (2013) 21064–21074.
- [21] X. Chen, T. Hou, K.A. Persson, Q. Zhang, *Mater. Today* 22 (2019) 142–158.
- [22] B. Chen, J. Ju, J. Ma, J. Zhang, R. Xiao, G. Cui, L. Chen, *Phys. Chem. Chem. Phys.* 19 (2017) 31436–31442.
- [23] A.M. Nolan, Y. Zhu, X. He, Q. Bai, Y. Mo, *Joule* 2 (2018) 2016–2046.
- [24] Y. Zhu, X. He, Y. Mo, *J. Mater. Chem. A* 4 (2016) 3253–3266.
- [25] Y. Zhu, X. He, Y. Mo, *ACS Appl. Mater. Interfaces* 7 (2015) 23685–23693.
- [26] F. Han, Y. Zhu, X. He, Y. Mo, C. Wang, *Adv. Energy Mater.* 6 (2016) 1501590.
- [27] W.D. Richards, L.J. Miara, Y. Wang, J.C. Kim, G. Ceder, *Chem. Mater.* 28 (2016) 266–273.
- [28] N. Ohta, K. Takada, L. Zhang, R. Ma, M. Osada, T. Sasaki, *Adv. Mater.* 18 (2006) 2226–2229.
- [29] D. Zhou, Y. Chen, B. Li, H. Fan, F. Cheng, D. Shanmukaraj, T. Rojo, M. Armand, G. Wang, *Angew. Chem. Int. Ed.* 57 (2018) 10168–10172.
- [30] Y.-S. Lee, J.H. Lee, J.-A. Choi, W.Y. Yoon, D.-W. Kim, *Adv. Funct. Mater.* 23 (2013) 1019–1027.
- [31] C. Wang, Q. Sun, Y. Liu, Y. Zhao, X. Li, X. Lin, M.N. Banis, M. Li, W. Li, K.R. Adair, D. Wang, J. Liang, R. Li, L. Zhang, R. Yang, S. Lu, X. Sun, *Nano Energy* 48 (2018) 35–43.
- [32] B. Xu, H. Duan, H. Liu, C.A. Wang, S. Zhong, *ACS Appl. Mater. Interfaces* 9 (2017) 21077–21082.
- [33] H.W. Kim, P. Manikandan, Y.J. Lim, J.H. Kim, S.-c. Nam, Y. Kim, *J. Mater. Chem. A* 4 (2016) 17025–17032.
- [34] L. Wang, Y. Wang, Y. Xia, *Energy Environ. Sci.* 8 (2015) 1551–1558.
- [35] J.-Y. Wu, S.-G. Ling, Q. Yang, H. Li, X.-X. Xu, L.-Q. Chen, *Chin. Phys. B* 25 (2016), 078204.
- [36] Q. Yu, D. Han, Q. Lu, Y.-B. He, S. Li, Q. Liu, C. Han, F. Kang, B. Li, *ACS Appl. Mater. Interfaces* 11 (2019) 9911–9918.
- [37] H. Gao, L. Xue, S. Xin, K. Park, J.B. Goodenough, *Angew. Chem. Int. Ed.* 56 (2017) 5541–5545.
- [38] Z. Zhang, Q. Zhang, J. Shi, Y.S. Chu, X. Yu, K. Xu, M. Ge, H. Yan, W. Li, L. Gu, Y.-S. Hu, H. Li, X.-Q. Yang, L. Chen, X. Huang, *Adv. Energy Mater.* 7 (2017) 1601196.
- [39] H. Kim, Y. Ding, P.A. Kohl, J. Power Sources 198 (2012) 281–286.
- [40] D.Y. Oh, Y.J. Nam, K.H. Park, S.H. Jung, S.-J. Cho, Y.K. Kim, Y.-G. Lee, S.-Y. Lee, Y.S. Jung, *Adv. Energy Mater.* 5 (2015) 1500865.
- [41] H. Duan, Y.-X. Yin, Y. Shi, P.-F. Wang, X.-D. Zhang, C.-P. Yang, J.-L. Shi, R. Wen, Y.-G. Guo, L.-J. Wan, *J. Am. Chem. Soc.* 140 (2018) 82–85.
- [42] Y. Gao, D. Wang, Y.-C. Li, Z. Yu, T.E. Mallouk, D. Wang, *Angew. Chem. Int. Ed.* 57 (2018) 13608–13612.
- [43] F. Aguesse, W. Manalastas, L. Buannic, J.M. Lopez del Amo, G. Singh, A. Llordés, J. Kilner, *ACS Appl. Mater. Interfaces* 9 (2017) 3808–3816.
- [44] Z. Zhang, S. Chen, J. Yang, J. Wang, L. Yao, X. Yao, P. Cui, X. Xu, *ACS Appl. Mater. Interfaces* 10 (2018) 2556–2565.
- [45] B. Zheng, J. Zhu, H. Wang, M. Feng, E. Umeshbabu, Y. Li, Q.-H. Wu, Y. Yang, *ACS Appl. Mater. Interfaces* 10 (2018) 25473–25482.
- [46] W. Dong, X.-X. Zeng, X.-D. Zhang, J.-Y. Li, J.-L. Shi, Y. Xiao, Y. Shi, R. Wen, Y.-X. Yin, T.-s. Wang, C.-R. Wang, Y.-G. Guo, *ACS Appl. Mater. Interfaces* 10 (2018) 18005–18011.
- [47] K. Xu, A. von Cresce, U. Lee, *Langmuir* 26 (2010) 11538–11543.
- [48] S. Shi, P. Lu, Z. Liu, Y. Qi, L.G. Hector, H. Li, S.J. Harris, *J. Am. Chem. Soc.* 134 (2012) 15476–15487.
- [49] M. Keller, A. Varzi, S. Passerini, *J. Power Sources* 392 (2018) 206–225.
- [50] L. Chen, L.Z. Fan, *Energy Storage Mater.* 15 (2018) 37–45.
- [51] S. Wenzel, S. Randau, T. Leichtweiss, D.A. Weber, J. Sann, W.G. Zeier, J. Janek, *Chem. Mater.* 28 (2016) 2400–2407.
- [52] H.-J. Peng, J.-Q. Huang, X.-B. Cheng, Q. Zhang, *Adv. Energy Mater.* 7 (2017) 1700260.
- [53] T. Doi, Y. Iriyama, T. Abe, Z. Ogumi, *Anal. Chem.* 77 (2005) 1696–1700.
- [54] T. Abe, F. Sagane, M. Ohtsuka, Y. Iriyama, Z. Ogumi, *J. Electrochem. Soc.* 152 (2005) A2151–A2154.
- [55] C. Pfaffenhuber, M. Göbel, J. Popovic, J. Maier, *Phys. Chem. Chem. Phys.* 15 (2013) 18318–18335.
- [56] T. Okumura, T. Fukutsuka, K. Matsumoto, Y. Oriksa, H. Arai, Z. Ogumi, Y. Uchimoto, *J. Phys. Chem. Lett.* C 115 (2011) 12990–12994.
- [57] X. He, Y. Zhu, Y. Mo, *Nat. Commun.* 8 (2017) 15893.
- [58] X. He, Y. Zhu, A. Epstein, Y. Mo, *NPJ Comput. Mater.* 4 (2018) 18.
- [59] D. Zheng, D. Qu, X.-Q. Yang, H.-S. Lee, D. Qu, *ACS Appl. Mater. Interfaces* 7 (2015) 19923–19929.
- [60] S. Uchida, M. Ishikawa, *J. Power Sources* 359 (2017) 480–486.
- [61] F. Sagane, T. Abe, Z. Ogumi, *J. Electrochem. Soc.* 159 (2012) A1766–A1769.
- [62] H. Valencia, M. Kohyama, S. Tanaka, H. Matsumoto, *J. Chem. Phys.* 131 (2009) 244705.
- [63] L. Wang, Z. Zhou, X. Yan, F. Hou, L. Wen, W. Luo, J. Liang, S.X. Dou, *Energy Storage Mater.* 14 (2018) 22–48.
- [64] J.B. Goodenough, Y. Kim, *Chem. Mater.* 22 (2010) 587–603.
- [65] P. Peljo, H.H. Girault, *Energy Environ. Sci.* 11 (2018) 2306–2309.
- [66] M.D. Radin, S. Hy, M. Sina, C. Fang, H. Liu, J. Vinckeviciute, M. Zhang, M.S. Whittingham, Y.S. Meng, A. Van der Ven, *Adv. Energy Mater.* 7 (2017) 1602888.
- [67] X.-Q. Zhang, C.-Z. Zhao, J.-Q. Huang, Q. Zhang, *Engineering* 4 (2018) 831–847.
- [68] M. Odzierskowski, D.E. Irish, *J. Electrochem. Soc.* 139 (1992) 3063–3074.
- [69] X.-Q. Zhang, X. Chen, L.-P. Hou, B.-Q. Li, X.-B. Cheng, J.-Q. Huang, Q. Zhang, *ACS Energy Lett.* 4 (2019) 411–416.
- [70] P. Schmitz, R. Jakelski, M. Pyschik, K. Jalkanen, S. Nowak, M. Winter, P. Bieker, *ChemSusChem* 10 (2017) 876–883.
- [71] P. Schmitz, M. Kolek, M. Pyschik, K. Jalkanen, S. Nowak, M. Winter, P. Bieker, *ChemistrySelect* 2 (2017) 6052–6056.
- [72] J. Saint, A.S. Best, A.F. Hollenkamp, J. Kerr, J.-H. Shin, M.M. Doeff, *J. Electrochem. Soc.* 155 (2008) A172–A180.
- [73] S. Xiong, K. Xie, E. Blomberg, P. Jacobsson, A. Matic, *J. Power Sources* 252 (2014) 150–155.
- [74] J.B. Haskins, H. Yildirim, C.W. Bauschlicher, J.W. Lawson, *J. Phys. Chem. Lett.* C 121 (2017) 28235–28248.
- [75] A.S. Best, A.I. Bhatt, A.F. Hollenkamp, *J. Electrochem. Soc.* 157 (2010) A903–A911.
- [76] A. Budi, A. Basile, G. Opletal, A.F. Hollenkamp, A.S. Best, R.J. Rees, A.I. Bhatt, A.P. O'Mullane, S.P. Russo, *J. Phys. Chem. Lett.* C 116 (2012) 19789–19797.
- [77] K. Edström, T. Gustafsson, J.O. Thomas, *Electrochim. Acta* 50 (2004) 397–403.
- [78] J. Cabana, B.J. Kwon, L. Hu, *Accounts Chem. Res.* 51 (2018) 299–308.
- [79] D. Aurbach, B. Markovsky, G. Salitra, E. Markevich, Y. Talyosoff, M. Koltypin, L. Nazar, B. Ellis, D. Kovacheva, *J. Power Sources* 165 (2007) 491–499.
- [80] M.R. Busche, T. Drossel, T. Leichtweiss, D.A. Weber, M. Falk, M. Schneider, M.-L. Reich, H. Sommer, P. Adelhelm, J. Janek, *Nat. Chem.* 8 (2016) 426.
- [81] J.H. Shin, W.A. Henderson, G.B. Appetecchi, F. Alessandrini, S. Passerini, *Electrochim. Acta* 50 (2005) 3859–3865.
- [82] H. Huo, N. Zhao, J. Sun, F. Du, Y. Li, X. Guo, *J. Power Sources* 372 (2017) 1–7.
- [83] B. Sun, K. Liu, J. Lang, M. Fang, Y. Jin, H. Wu, *Electrochim. Acta* 284 (2018) 662–668.
- [84] X. Hong, J. Mei, L. Wen, Y. Tong, A.J. Vasileff, L. Wang, J. Liang, Z. Sun, S.X. Dou, *Adv. Mater.* 31 (2019) 1802822.
- [85] Z. Zhang, L. Zhang, Y. Liu, H. Wang, C. Yu, H. Zeng, L.-m. Wang, B. Xu, *ChemSusChem* 11 (2018) 3774–3782.
- [86] C. de la Torre-Gamarra, G.B. Appetecchi, U. Ulissi, A. Varzi, A. Varez, S. Passerini, *J. Power Sources* 383 (2018) 157–163.
- [87] W. Lei, W. Xiaowei, L.G. Qiang, L.H. Ze, L. Ji, D.S. Xue, *Surf. Innov.* 6 (2018) 13–18.
- [88] W.-I. Qiu, X.-h. Ma, Q.-h. Yang, Y.-b. Fu, X.-f. Zong, *J. Power Sources* 138 (2004) 245–252.
- [89] Y. Cui, X. Liang, J. Chai, Z. Cui, Q. Wang, W. He, X. Liu, Z. Liu, G. Cui, J. Feng, *Adv. Sci.* 4 (2017) 1700174.
- [90] L. Kong, H. Zhan, Y. Li, Y. Zhou, *Electrochim. Commun.* 9 (2007) 2557–2563.
- [91] D. Zhou, Y.-B. He, R. Liu, M. Liu, H. Du, B. Li, Q. Cai, Q.-H. Yang, F. Kang, *Adv. Energy Mater.* 5 (2015) 1500353.
- [92] X. Li, K. Qian, Y.-B. He, C. Liu, D. An, Y. Li, D. Zhou, Z. Lin, B. Li, Q.-H. Yang, F. Kang, *J. Mater. Chem. A* 5 (2017) 18888–18895.
- [93] D. Zhou, R. Liu, Y.-B. He, F. Li, M. Liu, B. Li, Q.-H. Yang, Q. Cai, F. Kang, *Adv. Energy Mater.* 6 (2016) 1502214.
- [94] D. Zhou, Y.-B. He, Q. Cai, X. Qin, B. Li, H. Du, Q.-H. Yang, F. Kang, *J. Mater. Chem. A* 2 (2014) 20059–20066.
- [95] J. Amanokura, Y. Suzuki, S.-i. Imabayashi, M. Watanabe, *J. Electrochem. Soc.* 148 (2001) D43–D48.
- [96] Q. Xue, J. Li, G. Xu, H. Zhou, X. Wang, F. Kang, *J. Mater. Chem. A* 2 (2014) 18613–18623.
- [97] Y. Ma, J. Ma, J. Chai, Z. Liu, G. Ding, G. Xu, H. Liu, B. Chen, X. Zhou, G. Cui, L. Chen, *ACS Appl. Mater. Interfaces* 9 (2017) 41462–41472.
- [98] S. Wenzel, D.A. Weber, T. Leichtweiss, M.R. Busche, J. Sann, J. Janek, *Solid State Ion.* 286 (2016) 24–33.
- [99] Y. Gao, Z. Yan, J.L. Gray, X. He, D. Wang, T. Chen, Q. Huang, Y.C. Li, H. Wang, S.H. Kim, T.E. Mallouk, D. Wang, *Nat. Mater.* 18 (2019) 384–389.
- [100] S. Chen, C. Niu, H. Lee, Q. Li, L. Yu, W. Xu, J.-G. Zhang, E.J. Dufek, M.S. Whittingham, S. Meng, J. Xiao, J. Liu, *Joule* 3 (2019) 1094–1105.
- [101] C. Yan, X.-B. Cheng, Y. Tian, X. Chen, X.-Q. Zhang, W.-J. Li, J.-Q. Huang, Q. Zhang, *Adv. Mater.* 30 (2018) 1707629.
- [102] C. Yan, X.-B. Cheng, Y.-X. Yao, X. Shen, B.-Q. Li, W.-J. Li, R. Zhang, J.-Q. Huang, H. Li, Q. Zhang, *Adv. Mater.* 30 (2018) 1804461.